ARCHIVES of FOUNDRY ENGINEERING

ISSN (1897-3310)
Volume 9
Issue 2/2009
173-176

39/2

Published quarterly as the organ of the Foundry Commission of the Polish Academy of Sciences

Weld microstructure in cast AlSi9/SiC$_{(p)}$ metal matrix composites

J. Wysocki [a], K. Gawdzińska [b,*], S. Lenart [c]

[a] Polish Marine Service, Poland

[b] Institute of Basic Technical Sciences, Maritime Academy, ul. Podgórna 51/53, 70-205 Szczecin, Polska

[c] Institute of Materials Science and Engineering, Westpomeranian University of Technology, Al. Piastów 17, 70-310 Szczecin, Polska

*Contact: e-mail: kasiag@am.szczecin.pl

Received 26.02.2009; accepted in revised form: 30.03.2009

Abstract

Welded joint in cast AlSi9/SiC/20$_{(p)}$ metal matrix composite by manual TIG arc welding using AlMg5 filler metal has been described in his paper. Cooling curves have been stated, and the influence in distribution of reinforced particles on crystallization and weld microstructure. Welded joint mechanical properties have been determined: hardness and tensile.

Key words: cast AlSi9/SiC/20$_{(p)}$ composite, weld microstructure, cooling curves, mechanical properties

1. Introduction

Dynamic development in many industrial spheres is associated with researching modern technologies and materials. This is especially important nowadays in searching for the possibility of saving energy. In this aspect metal matrix composites appear very promising. Because of the relative ease and economy of fabrication, cast metal matrix composites based on aluminium-silicon alloys reinforced by silicon-carbon particles are more frequently being used in modern applications [1–3]. However, use of this type of material is limited by lack of effective joining methods. Results of aluminium metal matrix composites welded joints by arc welding [1, 3–7] show that the high heat energy of the process leads to degradation of reinforcing particles and changes of microstructure in the weld and heat effect zone, causing reduction in joint mechanical properties [5–8].

Trials were carried out welding cast AlSi9/SiC/20(p) metal matrix composite by manual TIG arc welding using AlMg5 filler metal. The purpose of these trials was to determine what influence the reinforced particles have on the crystallization process of the melted parent material and filler metal combination, and the mechanical properties of the weld.

2. Experimental procedure

Cast AlSi9/SiC/20(p) metal matrix composite used in trials. Chemical composition of parent material is shown in table I. Workpieces of 70×70×8 mm plates were cut from parent composite billet. Plate edges were slanted to form a single V – groove at 45°. In plates drilled slots at diam 2.5 mm, which were introduced 18/8 stainless steel casings. In purpose set cooling curves, in casings inserted K type thermocouples couplet with multiple temperature recorder Eurotherm 5100 V type. First thermocouple (S) was situated in wed gap symmetric line, second (P) and third (K) in parent respectively 2 and 4 mm material from slant surface. Thermocouples positions and workpiece diameters are shown in figure 1.

Table 1.
Chemical composition of parent material (% wt.)

Material	Si	Fe	Cu	Mn	Mg	Zn	Ti	Al
AlSi9+20%SiC	9.2%	0.14%	0.01%	0.01%	0.60%	0.02%	0.11%	bal.

Table 2.
Chemical composition of filler metal (% wt.)

Si	Fe	Cu	Mn	Mg	Cr	Zn	Ti	Al
0,25	0.4	0.05	0.1–0.2	4.5–5.5	0.1–0.2	0.1	0.15	bal.

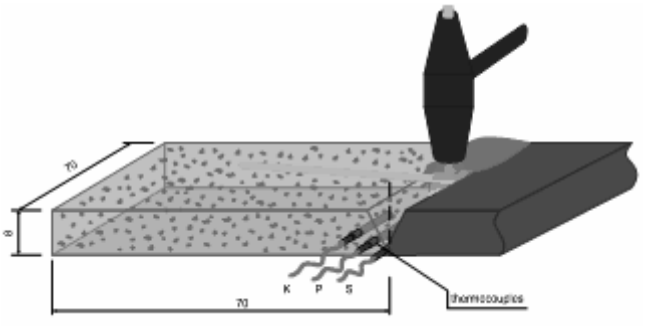

Fig. 1. Thermocouples positions and workpice dimensions

Using welding machine FALTIG 315 AC/DC, butt welds were performed in manual TIG arc welding process. Welds were made with one weld pass over a copper back plate. Welding conditions: current intensity A = 120 ampere (AC), welding speed v = 0.09m/min, shield gas argon with output V = 15 dm^3/min, inconsumable electrode tungsten Ø 2.4 mm, filler metal ER5356 (AlMg5) Ø 2.4 mm. Chemical composition of filler metal is shown in table II. Before welding workpieces were cleaned, degreased and heated to 150°C.

Welded joints obtained were cut perpendicular to weld axis. Specimens were ground with grid cabinet paper and finally polished using a felt disk wet with Al_2O_3 particulate suspension polishing liquid. Finally, specimens were degreased and etched by Keller solution. Microstructure was investigated using Neophot 2 optical microscope.

3. Results and discussion

3.1. Influence of cooling rate on weld microstructure

Weld solidification conditions were based on solidification time [9–12]. Cooling curves and their first derivatives are shown in fig. 2.

Cooling of welded joint course at room atmosphere. Crystallization of center part of weld started from nucleation dendrite of α phase at temperature about 655°C. Solidification process of α phase proceeded to temperature about 566°C, when α + Si eutectic nucleation occurred (A_s – fig. 2) which filled in interdendrite spaces. In interdenrite spaces small agglomerates of SiC were situated, rejected at the solid/liquid interface and pushed ahead by fast growing crystallization front [11–16]. Particles characterized by lower heat conductivity than surrounding metal matrix were reducing weld cooling process. Simultaneity they are a physical barrier for growing dendrite of α phase and diffusion of chemical elements at fusion line area. Hence it seem that small agglomerates of reinforced particles have privileged places of nucleation surrounded α + Si eutectic. At temperature 554°C nucleated triple eutectic phase α+Mg_2Si+Si where participation Mg_2Si phase on figure 3 is visible as "chinese letters". Solidification process finished at temperature 540°C (C_s – fig. 2).

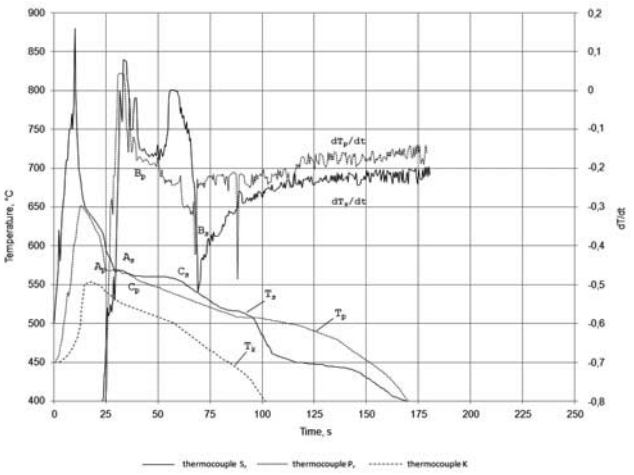

Fig. 2. Cooling curves and theirs first derivatives

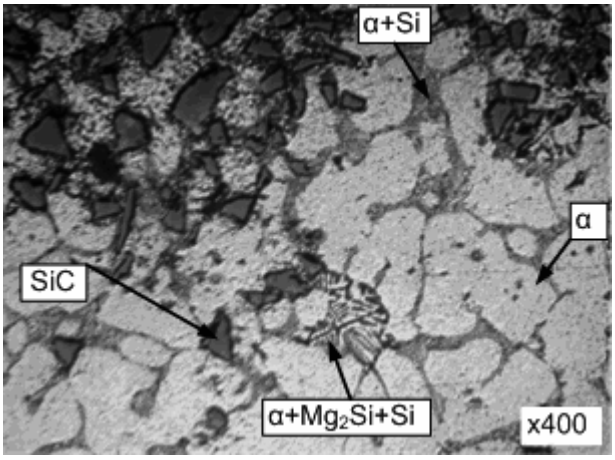

Fig. 3. Weld microstructure at center part – optical microscopy

The cooling curve has a somewhat different course at the fusion line area, where were different solidification conditions. Pronounced conglomeration of reinforced particles were noticed (fig. 4), which significantly limited growing of α phase grain. At temperature 570°C nucleated α+Si eutectic. Solidification process finished at temperature 533°C [14–15, 17–18].

Take into consideration that in point K there had been high heat transfer intensity and it was impossible to register temperature changes during crystallization process.

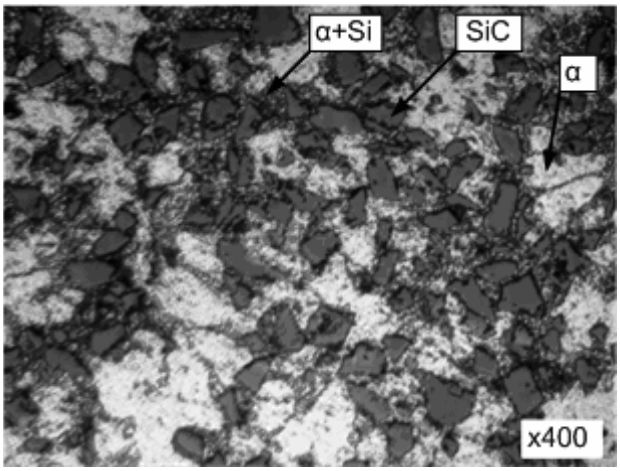

Fig. 4. Weld microstructure at the fusion line areas – optical microscopy

3.2. Welded joint mechanical properties

For welded joints a hardness profile has been determined and tensile tests carried out.

Hardness profile

The Vickers hardness test was performed using Shimadzu M tester with a load of 0.98 N (HV0.1), over a load time of exactly 10 s. The test was repeated five times and average values calculated using all results. The results of hardness tests are presented in figure 5.

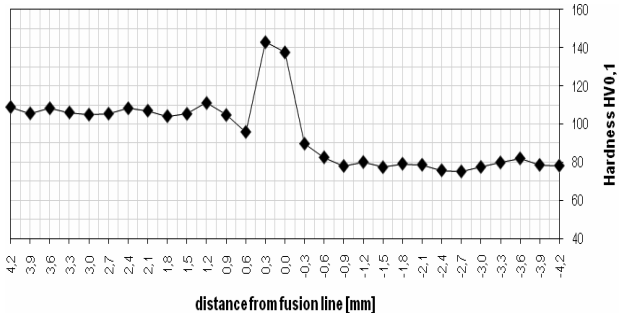

Fig. 5. Hardness profile

As is evident from the graph, hardness clearly increases at the fusion line area, where considerable agglomeration of reinforced particles has been noticed. Internal stress in the metal matrix during solidification process and a high proportion of eutectic phases can also have influence on the hardness in this area. It has been noticed that in area adjacent to the fusion line on the parent material side hardness dropped by about 10%. This is caused by the annealing effect made by the slower cooling of reinforced particles. However, the central part of the weld was characterized by an almost 20% reduction in hardness in comparison with the parent material [17–19]. It is the result of the growing dendrite grain of α phase in the area where there are a smaller numbers of reinforced particles.

Tensile strength

Specimens for tensile test were prepared based on Polish Norm PN-EN 10002-1 as non standard [3–4, 7, 10]. Specimens dimensions were shown on figure 6.

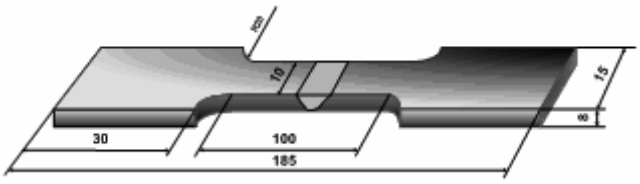

Fig. 6. Shape and specimen dimensions used for tensile test

Tensile tests were performed five times for welded joints and parent material. Average results are shown in table 3.

Table 3.
Welded joint and parent material tensile strength

Material	R_m [MPa]	ΔL_m [%]
AlSi9+20%SiC_p	168	3.34
Welded joint	137	2.94

Welded joints show an almost 20% drop of tensile strength in comparison with parent material. In all welded specimens, the failure occurred through the center part of weld (fig. 7a). Examination of the fracture surface edge by light microscopy (fig. 7b) shows that the fracture occurs at the border of dendrite grain of α phase where fragile α+Si eutectic are located. No surface damage was detected at particle/matrix interface, which proves good wetability of reinforced particles by metal matrix, and lack of brittle reaction products [7, 9, 10, 14–16].

4. Conclusions

Results obtained from welding metal matrix composites type AlSi/$SiC_{(p)}$ using ER5356 (AlMg5) filler metal by manual TIG welding process provides the following conclusions:

1. Reinforced particles have influence on weld cooling process and amount of precipitation phases in metal matrix.
2. The application of ER5356 (AlMg5) filler metal allowed good wetability of ceramic reinforced particles by metal matrix in weld formation process.
3. Growing of α phase grain in central part of weld where smaller number of reinforced particles are present and nucleation eutectic phases in interdendric spaces reduces welded joint mechanical properties.

a) b)

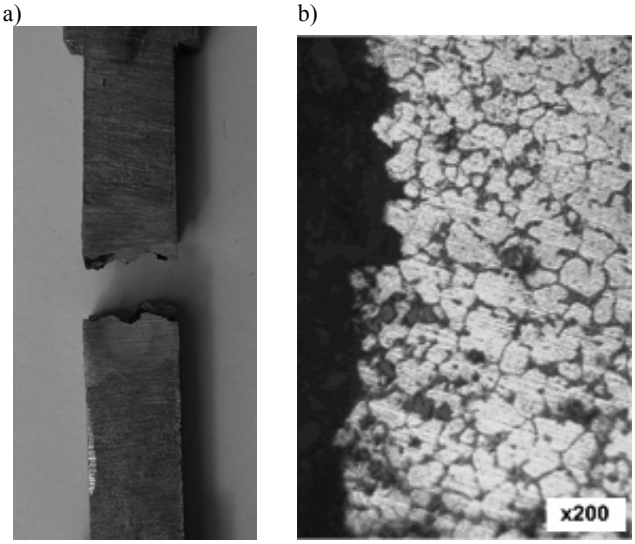

Fig. 7. a) fractured specimen of welded joint; b) microstructure of fracture surface edge – light microscopy

References

[1] J.M. Gomez de Salazar, M.I. Barrena, Dissimilar fusion welding of AA7020/MMC reinforced with Al_2O_3 particles and mechanical properties, Materials Science and Engineering A352 (2003) 162-168.

[2] P.P. Lean, L. Gil, A. Ureña, Dissimilar welds between unreinforced AA6082 and AA6092/SiC/25p composite by pulsed-MIG arc welding using unreinforced filler alloys (Al-5Mg and Al-5Si), Journal of Materials Processing Technology 143-144 (2003) 846-850.

[3] A. Chidambaram, S.D. Bhole, Particle Denuded Zones in Alumina Reinforced Aluminum Matrix Composite Weldments, Scripta Materiala, Vol. 35, No.3, pp. 373-378, 1996.

[4] G.G. Chernyshov, S.A. Paniczenko, T.A. Chernyshova, Welding of Metal Composites, Welding International, Vol. 17, no. 6, pp. 487-492, 2003. Selected from "Svarochnoe Proizvostvo" 50 (1), 26-31, 2003, Referance SP/03/1/26, Translation 3155.

[5] A. Orłowicz, M. Mróz, Study on susceptibility of Al-Si alloy castings to surface refinement with TIG arc, Zeitschrift für Meltrallkunde, t. 96, z. 12, s. 1391-1397, 2005.

[6] A. Orłowicz, A. Trytek, Kształtowanie mikrostruktury i właściwości użytkowych odlewów żeliwnych uszlachetnionych powierzchniowo plazmą łuku elektrycznego, monografia, Archiwum Odlewnictwa t. 7, z. 23, s. 1-120, 2007.

[7] M. Ottmuller, C. Korner, R.F. Singer, Influence of the fiber-matrix interface on the strength of unidirectional carbon fiber reinforced magnesium composites, Metal-Matrix Composites and Metallic Foams, 1999, Euromat'99, Vol.

[8] W. Orłowicz, Z. Opiekun, Kształtowanie struktury warstwy wierzchniej odlewów ze stopów kobaltu plazmą łuku elektrycznego, Biuletyn Instytutu Spawalnictwa Nr 5, 43-49, 2004.

[9] J. Grabian, J. Wysocki, TIG-bonding of AlSi9/SiC composites, Welding International 2007, 21 (4), 368-371.

[10] J. Grabian, K. Gawdzińska, J. Wysocki, Trial joint metal matrix composite by welding process. Kompozyty. Wybór prac Zachodniopomorskiego Oddziału Polskiego Towarzystwa Materiałów Kompozytowych. Szczecin 2003, str. 31-36 (in Polish).

[11] K. Gawdzińska, J. Hajkowski, B. Głowacki, Impact of Cooling Time on the Structure and Tribological Properties of Metal Matrix Composite Castings, Proceedings oh the Eighteenth (2008) International Offshore and Polar Engineering Conference Vancouver, Canada. July 6-11, 2008, s. 417-420.

[12] K. Gawdzińska, Discontinuities in metal composite cast materials. Archives of Foundry Engineering 13/1, 2007, vol. 7, s. 65-68.

[13] J. Piątkowski, The analysis of solidification and microstructure of Al-Si allos, Archiwum Odlewnictwa, 2006, vol. 6, Nr 18(1/2), pp. 364-369.

[14] S. Pietrowski, Characteristic features of silumin alloys crystallization, Materials & Design, 1997, Vol. 18, Nos. 4/6, pp. 379-383.

[15] J. Sakwa, Zur Kristallisation der Aluminiumguslegierung AlSi7Mg", Giessereiforschung, 1988, 4, 134.

[16] S. Wong, E. Neussl, D. Fettweis, O.R. Sahm, H.M.L. Flower, High strength Al-Zn-Mg matrix-alloy for continuous fibre reinforcement, [in:] Metal matrix composites and metallic foams, 2000, Euromat'2000; vol. 5, Wiley-Vch Verlag Gmbh 2000, pp. 119-127.

[17] M. Jovanovic, G. Rihar, J. Grum, Analysis of Ultrasonic Indications in Lack of Fusion Occurring in Welds, Proceedings of the 9th ECNDT, Berlin, 2006.

[18] S.J. Song, D.H. Kin, Precipitation behaviour of Mg17Al12 in SiC Particulate Reinforced Mg-Al-Zn Composite, Journal of the Korean Institute of Metals and Materials, 35 (11997) p. 351-358.

[19] D. Van Hille, S. Bengtsson, and R. Warren, Quantitative Metallographic Study of Fiber Morphology in a Short Fiber Al2O3 Fiber Reinforced Al Alloy Matrix, Comp. Sci. Tech., 35, 195-206 (1989).